55. M. Rusek and A. Orłowski, "Anderson localization of electromagnetic waves in confined dielectric media," *Phys. Rev. E* ***59***(3), 3655 (1999).

56. B. Souillard, "Waves and electrons in inhomogeneous media," in J. Souletie, J. Vannimenus, and R. Stora, Eds., *Chance and Matter*, North-Holland, Amsterdam, The Netherlands, 1987, p. 305.

CHAPTER SIX

Field Distribution, Anderson Localization, and Optical Phenomena in Random Metal–Dielectric Films

ANDREY K. SARYCHEV

Center for Applied Problems of Electrodynamics, 127412 Moscow, Russia

VLADIMIR M. SHALAEV

Department of Physics, New Mexico State University, Las Cruces, NM 88003

This chapter presents a theory of optical, infrared (IR), and microwave response of metal–dielectric inhomogeneous films. First, we describe the generalized Ohm's law approximation formulated for the case when the inhomogeneity length scale is much smaller than the wavelength, but is not smaller than the skin (penetration) depth for metal grains. In this approach, electric and magnetic fields *outside* a film are related to the currents *inside* the film. The computer simulations, based on the generalized Ohm's law approximation, reproduce the prominent absorption band near the percolation threshold and show that local electric and magnetic fields experience giant spatial fluctuations, which were detected in recent experiments. The fields are localized in small spatially separated peaks: electric and magnetic hot spots. A scaling theory, which is discussed in detail, predicts that the hot spots represent localized surface plasmons. The localization maps the Anderson transition problem, which is described by the random Hamiltonian with diagonal and off-diagonal disorder. The local fields exceed the applied field by several orders of magnitude, resulting in the enormous enhancement of various optical phenomena (Raman and hyper-Raman scattering, Kerr refraction, four-wave mixing, etc.). At percolation, a dip in the dependence of optical processes on the metal concentration is predicted. It is also shown that transmittance of a regular array of holes in a metal film is much enhanced when the incident wave is in resonance with one of the internal modes in the film.

Optics of Nanostructured Materials, Edited by Vadim A. Markel and Thomas F. George
ISBN 0-471-34968-2

6.1. INTRODUCTION

Random metal–dielectric films, also known as semicontinuous metal films, are usually produced by thermal evaporation or spattering of metal onto an insulating substrate. In the growing process, first, small clusters of metal grains are formed and, eventually, at a percolation threshold, a continuous conducting path appears between the ends of the sample, indicating a metal–insulator transition in the system. At high surface coverage, the film is mostly metallic with voids of irregular shape and, finally, the film becomes uniform. Over the past three decades, the electric transport properties of the semicontinuous metal films have been a topic of active experimental and theoretical study. The classical percolation theory had been employed to describe an anomalous behavior of the conductivity and other transport properties near the percolation threshold [1–4]. Recently, it was shown that quantum effects such as tunneling between metal clusters and electron localization become important at the percolation even at room temperature (see [5–8] and references cited therein). Thus low-frequency divergence of the dielectric constant was predicted theoretically [7,8] and then obtained experimentally [9].

In this chapter, we will consider the optical response of metal–insulator thin films that have been intensively studied both experimentally and theoretically along with transport phenomena (see, e.g., [3,4,10–22]). A two-dimensional (2D) nonhomogeneous film is a thin layer over which the local physical properties are not uniform. The response of such a layer to an incident wave depends crucially on the inhomogeneity length scale compared to the wavelength and also on the angle of incidence. Usually, when the wavelength is smaller than the inhomogeneity scale, the incident wave is scattered in various directions. The total field that is scattered in a certain direction is the sum of the elementary waves scattered in that direction by each elementary scatterer on the surface. As each elementary wave is given not only by its amplitude, but also by its phase, this sum will be a vector sum. The scattered wave is then distributed in various directions, though certain privileged directions may receive more energy than others. By contrast, when the inhomogeneity length scale is much smaller than the wavelength, the resolution of the wave is too small to "see" the irregularities, therefore the wave is then reflected specularly and transmitted in a well-defined direction, as if the film were a homogeneous layer with bulk effective physical properties (conductivity, permittivity, and permeability) that are uniform. The wave is coupled to the inhomogeneities in such a way that irregular currents are excited on the surface of the layer. Strong distortions of the field then appear near the surface; however, they decay exponentially so that far enough from the surface the wave resumes its plane wave character.

The question of scattering from a nonhomogeneous surface has attracted attention since the time of Lord Rayleigh [23]. Due to the wide range of potential applications in, for example, radiowave and radar techniques, most efforts have been concentrated in the regime where the scale of inhomogeneity is larger than the wavelength [24]. In the last decade, a problem of localization of surface polaritons [25] and other "internal modes" due to their interaction with surface roughness attracted a lot of attention. This localization was found to contribute a maximum to

the angular dependence of the intensity of the nonspecularly reflected light in the antispecular direction [26] and other "resonance directions" [27,28] as well. The development of near-field scanning optical microscopy has opened the way to probe the surface polariton field above the surface and visualize its distribution. Vast progress in the near-field optics of various rough surfaces and metal grain structures is discussed in Chapter 3. The subject of this chapter belongs to another regime, where the inhomogeneity length scale is much smaller than the wavelength, but can be of the order or even larger than skin depth. In other words, coupling of a metal grain with an *electromagnetic* (EM) field is supposed to be strong in spite of its subwavelength size. In particular, we focus on the high-frequency response (optical, IR, and microwave) of thin, metal-dielectric random films.

The optical properties of metal–dielectric films show anomalous phenomena that are absent for bulk metal and dielectric components. For example, the anomalous absorption in the near-IR spectral range leads to unusual behavior of transmittance and reflectance. Typically, the transmittance is much higher than that of continuous metal films, whereas the reflectance is much lower (see, e.g., [3,4,10,11,16–18]). Near and well below the percolation threshold, the anomalous absorbance can be as high as 50% [12–16,20]. A number of theories were proposed for calculation of the optical properties of semicontinuous random films, including the effective-medium approaches [29,30], their various modifications [3,16,17,31–35], and the renormalization group method (see e.g., [4,36,37]). In most of these theories, the semicontinuous metal–dielectric film is considered as a fully 2D system and quasistatic approximation is invoked. However, usage of that approximation implies that both the electric and magnetic fields in the film are assumed to be 2D and curl-free. That assumption ceases to be valid when the fields are changed considerably in the physical film and in its close neighborhood, which is usually the case in a semicontinuous metal thin film, especially in the strong skin effect regime.

In an attempt to expand the theoretical treatment beyond the quasistatic approximation, an approach was recently proposed that was based on the full set of Maxwell's equations [18–20]. This approach does not use the quasistatic approximation because the fields are not assumed to be curl-free inside the physical film. Although that theory was proposed with metal–insulator thin films in mind, it is in fact quite general and can be applied to any kind of inhomogeneous film under appropriate conditions. For reasons that will be explained below, this theory is called the "generalized Ohm's law" (GOL). We present this new theory here.

Below, we restrict ourselves to the case where all the external fields are parallel to the plane of the film. This means that an incident wave, as well as the reflected and transmitted waves, are traveling in the direction perpendicular to the film plane. We focus our attention on the electric and magnetic field magnitudes at certain distances *away* from the film and relate them to the currents *inside* the film. We assume that inhomogeneities on a film are much smaller in size than the wavelength λ (but not necessarily smaller than the skin depth), so that the fields away from the film are curl-free and can be expressed as gradients of potential fields. The electric and magnetic induction currents averaged over the film thickness obey the usual 2D continuity equations. Therefore, the equations for the fields (e.g., $\nabla \times \mathbf{E} =$

and the equations for the currents (e.g., $\nabla \cdot \mathbf{j} = 0$) are the *same* as in the quasistatic case. The only difference is that the fields and the averaged currents are now related by new constitutive equations and that there are magnetic as well as electric currents.

To determine these new constitutive equations, we find the electric and magnetic field distributions inside the conductive and dielectric regions of the film. The boundary conditions completely determine solutions of Maxwell's equations for the fields inside a grain when the frequency is fixed. Therefore the internal fields, which change very rapidly with position in the direction perpendicular to the film, depend linearly on the electric and magnetic field away from the film. The currents inside the film are linear functions of the local internal fields given by the usual local constitutive equations. Therefore, the currents flowing *inside* the film also depend linearly on the electric and magnetic fields *outside* the film. However, the electric current averaged over the film thickness now depends not only on the external electric field, but also on the external magnetic field. The same is true for the average magnetic induction current. Thus we have two linear equations that connect the two types of average internal currents to the external fields. These equations can be considered as a generalization of Ohm's law to the nonquasistatic case and they dub as GOL [19]. The GOL forms the basis of a new approach to calculate the EM properties of inhomogeneous films.

The continuity equations for the electric and magnetic currents use the GOL and take into account the potential character of the electric and magnetic fields outside the film. This allows us to determine the field and current distribution over a metal–dielectric film in the computer experiment, and, finally, to calculate the optical properties of the film. Computer simulations show that the local electric and magnetic fields both fluctuate strongly over the film at the metal concentration close to the percolation threshold. The fields are localized in small spatially separated peaks: electric and magnetic hot spots. When the skin effect in the metal grains is strong, the magnetic fluctuations are as large as fluctuations of the local electric field. The amplitude of local field fluctuations in the case of a strong skin effect is large regardless of losses in the metal. It is also important to note that giant magnetic field fluctuations is a purely nonquasistatic effect that cannot be obtained within the traditional approach used earlier.

We present a scaling theory of local field fluctuations in the random semicontinuous metal films [38–46]. The theory is based on the fact that the problem of optical excitations in semicontinuous metal films mathematically maps the Anderson transition problem. This allowed us to predict localization of surface plasmons in the films and to describe in detail the localization pattern. It is shown that the surface plasmons eigenstates are localized on a scale much smaller than the wavelength of the incident light. The surface plasmons eigenstates, with eigenvalues close to zero (resonant modes), are excited most efficiently by the external field. Since the eigenstates are localized and only a small portion of them are excited by the incident wave, the overlapping of the eigenstates can typically be neglected, which significantly simplifies theoretical consideration and allows one to obtain relatively simple expressions for the local field fluctuations. It is important to stress

that the surface plasmon localization length is much smaller than the wavelength; in that sense, the predicted subwavelength localization of the surface plasmons quite differs from the long-time discussed localization of light due to strong scattering in a random homogeneous medium [6,47].

The developed scaling theory of local field fluctuations in semicontinuous metal films opens up new means to study the classical Anderson problem by taking advantage of unique characteristics of laser radiation, namely, its coherence and high intensity. For example, this theory predicts that at percolation there is a *minimum* in nonlinear optical responses of metal–dielectric composites, a fact that follows from the Anderson localization of surface plasmon modes and can be studied and verified in laser experiments.

The rest of this chapter is organized as follows: the GOL for semicontinuous metal films is derived in Section 6.2. In Section 6.3, it is shown how the optical properties: (reflectance, transmittance, and absorbance) are found in the GOL approximation. The original computer method and calculation of the local electric and magnetic field are presented in Section 6.4. In Section 6.5 and 6.6, analytical theory is developed for the giant local field fluctuations. In Section 6.7, the theoretical results are implemented to find equations for the spatial moments of the local fields. In Section 6.8, we consider optical properties of a metal film that is perforated with an array of subwavelength holes; we show here that the transmittance through such a film can be strongly enhanced in agreement with recent experimental observations. Section 6.9 summarizes and concludes this chapter.

6.2. GOL AND BASIC EQUATIONS

We base the following presentation on the results of [18–20]. In contrast to the traditional consideration, it is not assumed that the electric and magnetic fields inside a semicontinuous metal film are curl-free and z independent, where the z coordinate is perpendicular to the film plane.

First, let us consider a homogeneous conducting film with a uniform conductivity σ_m and thickness d, and assume constant values of the electric field $\mathbf{E}_1$ and magnetic field $\mathbf{H}_1$ at some reference plane $z = -d/2 - \ell_0$ behind the film, as shown in Fig. 6.1. Under these conditions the fields depend only on the z coordinate, and Maxwell's equations for a monochromatic field can be written in the following form:

$$\frac{d}{dz}\mathbf{E}(z) = -\frac{i\omega}{c}\,\mu(z)[\mathbf{n} \times \mathbf{H}(z)] \tag{6.1}$$

$$\frac{d}{dz}\mathbf{H}(z) = -\frac{4\pi}{c}\,\sigma(z)[\mathbf{n} \times \mathbf{E}(z)] \tag{6.2}$$

with boundary conditions

$$\mathbf{E}(z = -d/2 - l_0) = \mathbf{E}_1 \qquad \mathbf{H}(z = -d/2 - l_0) = \mathbf{H}_1 \tag{6.3}$$

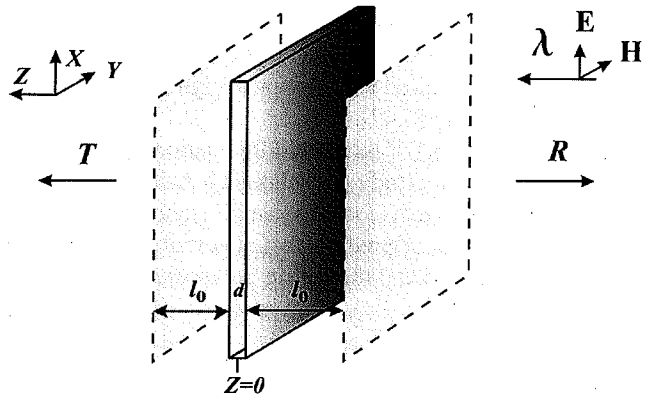

Figure 6.1. The scheme used in a theoretical model. Electromagnetic wave of wavelength λ is incident on a thin-metal–insulator film with thickness d. It is partially reflected and absorbed, and the remainder is transmitted through the film. The amplitudes of the electric and magnetic fields, which are averaged over the plane $z = -d/2 - l_0$ behind the film, are equal to each other.

where $\mathbf{E}_1$ and $\mathbf{H}_1$ are parallel to the film plane. Here, the conductivity $\sigma(z)$ is equal to the metal conductivity σ_m inside the film $(-d/2 < z < d/2)$ and to $\sigma_d = -i\omega/4\pi$ outside the film ($z < -d/2$ and $z > d/2$), and similarly, the magnetic permeability $\mu(z)$ is equal to the film permeability μ_m inside the film and to one outside the film; the unit vector $\mathbf{n} = (0, 0, 1)$ is perpendicular to the film plane. When solving Eqs. (6.1) and (6.2), it is taken into account that the electric and magnetic fields are continuous at the film boundaries. In this way, the fields $\mathbf{E}(z)$ and $\mathbf{H}(z)$ are determined everywhere. Then, electric $\mathbf{j}_E$ and magnetic $\mathbf{j}_H$ currents flowing in between the two planes at $z = -d/2 - l_0$ and at $z = d/2 + l_0$ are calculated as

$$\mathbf{j}_E = -\frac{i\omega}{4\pi}\left[\int_{-d/2-l_0}^{-d/2}\mathbf{E}(z)dz + \int_{-d/2}^{d/2}\varepsilon_m\mathbf{E}(z)dz + \int_{d/2}^{d/2+l_0}\mathbf{E}(z)dz\right] \tag{6.4}$$

$$\mathbf{j}_H = \frac{i\omega}{4\pi}\left[\int_{-d/2-l_0}^{-d/2}\mathbf{H}(z)dz + \int_{-d/2}^{d/2}\mu_m\mathbf{H}(z)dz + \int_{d/2}^{d/2+l_0}\mathbf{H}(z)dz\right] \tag{6.5}$$

where $\varepsilon_m = 4i\pi\sigma_m/\omega$ is the metal dielectric constant. In what follows, it is assumed, for simplicity, that the magnetic permeability $\mu_m = 1$. Since the Maxwell equations are linear, the local fields $\mathbf{E}(z)$ and $\mathbf{H}(z)$ are linear functions of the boundary values $\mathbf{E}_1$ and $\mathbf{H}_1$ defined at the plane $z = -d/2 - l_0$

$$\mathbf{E}(z) = a(z)\mathbf{E}_1 + c(z)[\mathbf{n} \times \mathbf{H}_1] \tag{6.6}$$

$$\mathbf{H}(z) = b(z)\mathbf{H}_1 + d(z)[\mathbf{n} \times \mathbf{E}_1] \tag{6.7}$$

Note that $\mathbf{n}$ is the single constant vector in the problem, which let us to build polar $[\mathbf{n} \times \mathbf{H}_1]$ and axial $[\mathbf{n} \times \mathbf{E}_1]$ vectors in Eqs. (6.6) and (6.7). By substituting Eq. (6.6) for $\mathbf{E}(z)$ and Eq. (6.7) for $\mathbf{H}(z)$ in Eqs. (6.4) and (6.5), we express the currents $\mathbf{j}_E$ and $\mathbf{j}_H$ in terms of the boundary (surface) fields $\mathbf{E}_1$ and $\mathbf{H}_1$ as

$$\mathbf{j}_E = s\mathbf{E}_1 + g_1\,[\mathbf{n} \times \mathbf{H}_1] \tag{6.8}$$

$$\mathbf{j}_H = m\mathbf{H}_1 + g_2\,[\mathbf{n} \times \mathbf{E}_1] \tag{6.9}$$

In contrast to the usual constitutive equations, the planar electric current $\mathbf{j}_E$, which flows between the planes $z = -d/2 - l_0$ and $z = d/2 + l_0$, depends not only on the external electric field $\mathbf{E}_1$ but also on the external magnetic field $\mathbf{H}_1$. The same is true for the magnetic induction current $\mathbf{j}_H$. These equations constitute the GOL. The Ohmic parameters s, m, g_1, and g_2 have the dimension of surface conductivity (cm/s) and depend on the frequency ω, the metal dielectric constant ε_m, the film thickness d, and the distance l_0 between the film and the reference plane $z = -d/2 - l_0$. Below, the films are supposed to be invariant under reflection through the plane $z = 0$. In this case, $g_1 = g_2 = g$ as it is shown in [18], and the Ohmic parameter g can be expressed in terms of parameters s and m as

$$g = -\frac{c}{4\pi} + \sqrt{\left(\frac{c}{4\pi}\right)^2 - ms} \tag{6.10}$$

Then, the GOL equations (6.8) and (6.9) take the following form:

$$\mathbf{j}_E = s\mathbf{E}_1 + g\,[\mathbf{n} \times \mathbf{H}_1] \tag{6.11}$$

$$\mathbf{j}_H = m\mathbf{H}_1 + g\,[\mathbf{n} \times \mathbf{E}_1] \tag{6.12}$$

where the Ohmic parameter g is given by Eq. (6.10). The Ohmic parameters s and m can be expressed in terms of the film refractive index $n = \sqrt{\varepsilon_m}$ and film thickness d in the following way:

$$s = \frac{c}{8n\pi}\left[e^{-idkn}(n\cos(adk) - i\sin(adk))^2 - e^{idkn}(n\cos(adk) + i\sin(adk))^2\right] \tag{6.13}$$

$$m = \frac{c}{8n\pi}\left[e^{-idkn}(i\cos(adk) + n\sin(adk))^2 - e^{idkn}(-i\cos(adk) + n\sin(adk))^2\right] \tag{6.14}$$

where we still assume, for simplicity, that $\varepsilon = 1$ outside the film $(z < -d/2$, $z > d/2)$ and introduce the wave vector $k = \omega/c$ and dimensionless parameter $a \equiv l_0/d$ (see [18,19]). The skin (penetration) depth δ is equal to $\delta = 1/k\,\mathrm{Im}\,n$ in these notations. In the microwave spectral range, metal conductivity is real and the dielectric constant ε_m is purely imaginary and the skin depth $\delta = c/\sqrt{2\pi\sigma_m\omega}$. On

the other hand, the dielectric constant is negative for a typical metal in the optical and IR spectral ranges, therefore $\delta \cong 1/k\sqrt{|\varepsilon_m|}$ in this case

We now turn to the case of laterally inhomogeneous films. Then, the currents $\mathbf{j}_E$ and $\mathbf{j}_H$ defined by Eqs. (6.4) and (6.5), as well as the fields $\mathbf{E}_1$ and $\mathbf{H}_1$, are functions of the 2D vector $\mathbf{r} = \{x, y\}$. From Maxwell's equations, it follows that the fields and currents are connected by linear relations

$$\mathbf{j}_E(\mathbf{r}) = s\mathbf{E}_1 + g\,[\mathbf{n} \times \mathbf{H}_1] \tag{6.15}$$

$$\mathbf{j}_H(\mathbf{r}) = m\mathbf{H}_1 + g\,[\mathbf{n} \times \mathbf{E}_1] \tag{6.16}$$

where s, m, and g are some integral operators now. The metal islands in semicontinuous films usually have an oblate shape so that the grain diameter D is much larger than the film thickness d (see, e.g., [11]). When the thickness of a conducting grain d (or skin depth δ) and distance l_0 are much smaller than the grain diameter D, the relation of the fields $\mathbf{E}_1$ and $\mathbf{H}_1$ to the currents becomes fully local in Eqs. (6.15) and (6.16). The local Ohmic parameters $s = s(\mathbf{r})$, $m = m(\mathbf{r})$, and $g = g(\mathbf{r})$, given by Eqs. (6.10), (6.13), and (6.14), are determined by the local refractive index $n(\mathbf{r}) = \sqrt{\varepsilon(\mathbf{r})}$, where $\varepsilon(\mathbf{r})$ is a local dielectric constant. Equations (6.15) and (6.16) are the local GOL for semicontinuous films. For binary metal–dielectric semicontinuous films, the local dielectric constant is equal to either ε_m or ε_d. The electric $\mathbf{j}_E$ and magnetic $\mathbf{j}_H$ currents given by Eqs. (6.15) and (6.16) lie in between the planes $z = -d/2 - l_0$ and $z = d/2 + l_0$. These currents satisfy the 2D continuity equations

$$\nabla \cdot \mathbf{j}_E(\mathbf{r}) = 0 \qquad \nabla \cdot \mathbf{j}_H(\mathbf{r}) = 0 \tag{6.17}$$

which follow from the three-dimensional (3D) continuity equations when the z components of $\mathbf{E}_1$ and $\mathbf{H}_1$ are neglected at the planes $z = \pm(d/2 + l_0)$. This is possible because these components are small, in accordance with the fact that the average fields $\langle \mathbf{E}_1 \rangle$ and $\langle \mathbf{H}_1 \rangle$ are parallel to the film plane. Since we consider semicontinuous films with an inhomogeneity scale much smaller than the wavelength λ, the fields $\mathbf{E}_1(\mathbf{r})$ and $\mathbf{H}_1(\mathbf{r})$ are still the gradients of potential fields when considered as functions of x and y in the fixed reference plane $z = -d/2 - l_0$, that is,

$$\mathbf{E}_1(\mathbf{r}) = -\nabla\varphi_1(\mathbf{r}) \qquad \mathbf{H}_1(\mathbf{r}) = -\nabla\psi_1(\mathbf{r}) \tag{6.18}$$

By substituting these expressions in the continuity Eq. (6.17) and taking into account the GOL Eqs. (6.15) and (6.16), the system of two basic equations for the electric φ_1 and magnetic ψ_1 potentials are obtained

$$\nabla \cdot (s\nabla\varphi_1 + g[\mathbf{n} \times \nabla\psi_1]) = 0 \qquad \nabla \cdot (m\nabla\psi_1 + g[\mathbf{n} \times \nabla\varphi_1]) = 0 \tag{6.19}$$

where all variables are functions of the coordinates x and y in the reference plain. The above equations must be solved under the following conditions:

$$\langle \nabla\varphi_1 \rangle = \langle \mathbf{E}_1 \rangle \qquad \langle \nabla\psi_1 \rangle = \langle \mathbf{H}_1 \rangle \tag{6.20}$$

where the constant fields $\langle \mathbf{E}_1 \rangle$ and $\langle \mathbf{H}_1 \rangle$ are external (given) fields. Here and below $\langle \cdots \rangle$ denotes an average over coordinates "x" and "y".

The essence of the GOL can be summarized as follows. The entire physics of a 3D inhomogeneous layer, which is described by the full set of Maxwell's equations, has been reduced to a set of quasistatic equations in a (2D) reference plane. Part of the price for this achievement is the introduction of coupled electric and magnetic fields, currents, and dependence on one adjustable parameter, namely, the distance l_0 to the reference plane. Comparison of the numerical calculation and the GOL approximation for the metal film with periodic corrugation [19] shows that GOL results are generally not sensitive to the distance l_0. The original choice $l_0 = 0.25\,D$ [18] [i.e., parameter $a = D/4d$ in Eqs. (6.13) and (6.14)] allows us to reproduce most of the computer simulations except those where a surface polariton is excited in the corrugated film.

6.3. DECOUPLING GOL EQUATIONS AND EFFECTIVE MEDIUM APPROXIMATION FOR TRANSMITTANCE, REFLECTANCE, AND ABSORBANCE

To simplify the system of the basic equations (6.19) the electric and magnetic fields on both sides of the film are considered [19,20]. Namely, the electric and magnetic fields are considered at the distance l_0 behind the film $\mathbf{E}_1(\mathbf{r}) = \mathbf{E}(\mathbf{r},\ -d/2 - l_0)$, $\mathbf{H}_1(\mathbf{r}) = \mathbf{H}(\mathbf{r},\ -d/2 - l_0)$, and at the distance l_0 in front of the film $\mathbf{E}_2(\mathbf{r}) = \mathbf{E}(\mathbf{r},\ d/2 + l_0)$, $\mathbf{H}_2(\mathbf{r}) = \mathbf{H}(\mathbf{r},\ d/2 + l_0)$. Remember that $\mathbf{r} = \{x,\ y\}$ is a 2D vector in a plane perpendicular to the "z" axis. The components of the fields aligned with z are still neglected. Then, the second Maxwell's equation curl $\mathbf{H} = (4\pi/c)\mathbf{j}$ can be written as $\oint \mathbf{H}d\mathbf{l} = (4\pi/c)\mathbf{j}_E\Delta$, where the integration is over the contour $ABCD$ shown in Fig. 6.2, while the current $\mathbf{j}_E$ is given by the GOL Eq. (6.15). When $\Delta \to 0$ this equation takes the following form

$$\mathbf{H}_2 - \mathbf{H}_1 = -\frac{4\pi}{c}\,[\mathbf{n} \times \mathbf{j}_E] = -\frac{4\pi}{c}\,(s[\mathbf{n} \times \mathbf{E}_1] - g\mathbf{H}_1) \tag{6.21}$$

When the same procedure is applied to the first Maxwell equation, curl $\mathbf{E} = ik\mathbf{H}$, it gives

$$\mathbf{E}_2 - \mathbf{E}_1 = -\frac{4\pi}{c}\,[\mathbf{n} \times \mathbf{j}_H] = -\frac{4\pi}{c}\,(m[\mathbf{n} \times \mathbf{H}_1] - g\mathbf{E}_1) \tag{6.22}$$

where the GOL equation (6.16) has been substituted for the electric current $\mathbf{j}_H$ in Eq. (6.22). Then, electric field $\mathbf{E}_1$ can be expressed from Eq. (6.21) in terms of the magnetic fields $\mathbf{H}_1$ and $\mathbf{H}_2$ as

$$[\mathbf{n} \times \mathbf{E}_1] = \frac{g}{s}\,\mathbf{H}_1 - \frac{c}{4\pi s}\,(\mathbf{H}_2 - \mathbf{H}_1) \tag{6.23}$$

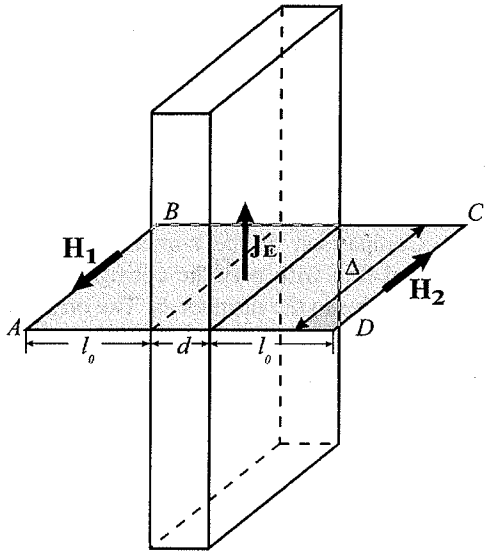

Figure 6.2. The left-hand side of the Maxwell's equation $\oint \mathbf{H}\, d\mathbf{l} = (4\pi/c)\mathbf{j}_E\Delta$ is integrated over the contour ABCD to obtain Eq. (6.21).

and the magnetic field $\mathbf{H}_1$ can be expressed from Eq. (6.22) in terms of the electric fields $\mathbf{E}_1$ and $\mathbf{E}_2$ as

$$[\mathbf{n} \times \mathbf{H}_1] = \frac{g}{m}\,\mathbf{E}_1 - \frac{c}{4\pi m}\,(\mathbf{E}_2 - \mathbf{E}_1) \tag{6.24}$$

Substitution the right-hand side (rhs) of Eq. (6.23) in the GOL Eq. (6.16) and substitution (6.24) in the GOL Eq. (6.15) results in

$$\mathbf{j}_E = s\mathbf{E}_1 + g\Big(\frac{g}{m}\,\mathbf{E}_1 - \frac{c}{4\pi m}\,(\mathbf{E}_2 - \mathbf{E}_1)\Big) \tag{6.25}$$

$$\mathbf{j}_H = m\mathbf{H}_1 + g\Big(\frac{g}{s}\,\mathbf{H}_1 - \frac{c}{4\pi s}\,(\mathbf{H}_2 - \mathbf{H}_1)\Big) \tag{6.26}$$

Finally, the relation (6.10) between the Ohmic parameters s, m, and g allows us to rewrite the above equations as

$$\mathbf{j}_E = u\mathbf{E} \qquad \mathbf{j}_H = w\mathbf{H} \tag{6.27}$$

where $\mathbf{E} = (\mathbf{E}_1 + \mathbf{E}_2)/2$, $\mathbf{H} = (\mathbf{H}_1 + \mathbf{H}_2)/2$ and parameters u and w are given by the following equations:

$$u = -\frac{c}{2\pi}\,\frac{g}{m} \qquad w = -\frac{c}{2\pi}\,\frac{g}{s} \tag{6.28}$$

Thus the GOL is diagonalized by introducing new fields $\mathbf{E}$ and $\mathbf{H}$ so that Eqs. (6.27) have the same form as constitutive equations of the macroscopic electrodynamics. The only difference is that the local conductivity σ is replaced by parameter u, and magnetic permeability μ is replaced by parameter $-i4\pi w/\omega$.

It follows from Eqs. (6.28) and (6.10), (6.13), and (6.14) that the new Ohmic parameters u and v are expressed in terms of the local refractive index $n = \sqrt{\varepsilon(\mathbf{r})}$ as

$$u = -i\,\frac{c}{2\pi}\,\frac{\tan(Dk/4) + n\,\tan(dkn/2)}{1 - n\,\tan(Dk/4)\,\tan(dkn/2)} \tag{6.29}$$

$$w = i\,\frac{c}{2\pi}\,\frac{n\,\tan(Dk/4) + \tan(dkn/2)}{n - \tan(Dk/4)\,\tan(dkn/2)} \tag{6.30}$$

where the parameter $a = D/4d$ is substituted as it is discussed at the end of Section 6.2. The refractive index n in the above equations takes values $n_m = \sqrt{\varepsilon_m}$ and $n_d = \sqrt{\varepsilon_d}$ for metal and dielectric regions of the film, respectively. In the quasistatic limit, when the optical thickness of metal grains is small, $dk|n_m| \ll 1$, while the metal dielectric constant is large in magnitude, $|\varepsilon_m| \gg 1$, the following estimates hold:

$$u_m \simeq -i\,\frac{\omega\varepsilon_m}{4\pi}\,d \qquad w_m \simeq i\,\frac{\omega}{4\pi}\,(d + D/2) \qquad (d/\delta \ll 1) \tag{6.31}$$

for the metal grains. In the opposite case of strong skin effect, when the skin depth (penetration depth) $\delta = 1/k\ \mathrm{Im}\, n_m$ is much smaller than the grain thickness d and the electromagnetic field does not penetrate in metal grains, the parameters u_m and w_m take values

$$u_m = i\,\frac{2c^2}{\pi D\omega} \qquad w_m = i\,\frac{\omega D}{8\pi} \qquad (d/\delta \gg 1) \tag{6.32}$$

For the dielectric region, when the film is thin enough so that $dkn_d \ll 1$ and $\varepsilon_d \sim 1$, Eqs. (6.29) and (6.30) give

$$u_d = -i\,\frac{\omega\varepsilon'_d}{8\pi}\,D \qquad w_d = i\,\frac{\omega}{4\pi}\,(d + D/2) \tag{6.33}$$

where the reduced dielectric constant $\varepsilon'_d = 1 + 2\varepsilon_d d/D$ is introduced. Note that in the limit of the strong skin effect the Ohmic parameters u_m and w_m are purely imaginary and the parameter u_m is of inductive character, that is, it has the sign opposite to the dielectric parameter u_d. In contrast, the Ohmic parameter w remains essentially the same $w \sim iD\omega/8\pi$ for dielectric and for metal regions regardless of the value of the skin effect.

Potentials for the fields $\mathbf{E}_2(\mathbf{r})$ and $\mathbf{H}_2(\mathbf{r})$ can be introduced for the same reason as potentials for the fields $\mathbf{E}_1(\mathbf{r})$ and $\mathbf{H}_1(\mathbf{r})$ [see the discussion accompanying

Eq. (6.18)]. Therefore the fields $\mathbf{E}(\mathbf{r})$ and $\mathbf{H}(\mathbf{r})$ in Eqs. (6.27) can in turn be represented as gradients of some potentials:

$$\mathbf{E} = -\nabla\phi' \qquad \mathbf{H} = -\nabla\psi' \tag{6.34}$$

By substituting these expressions into Eq. (6.27) and then into the continuity Eq. (6.17), we obtain the following equations:

$$\nabla \cdot [u(\mathbf{r})\nabla\varphi'(\mathbf{r})] = 0 \tag{6.35}$$
$$\nabla \cdot [w(\mathbf{r})\nabla\psi(\mathbf{r})] = 0 \tag{6.36}$$

which can be solved independently for the potentials φ' and ψ'. Eqs. (6.35) and (6.36) are solved under the following conditions:

$$\langle\nabla\varphi_1'\rangle = \langle\mathbf{E}\rangle \equiv \mathbf{E}_0 \qquad \langle\nabla\psi_1'\rangle = \langle\mathbf{H}_1\rangle \equiv \mathbf{H}_0 \tag{6.37}$$

where the constant fields $\mathbf{E}_0$ and $\mathbf{H}_0$ are external (given) fields that are determined by the incident wave. When the fields $\mathbf{E}$, $\mathbf{H}$ and currents $\mathbf{j}_E$, $\mathbf{j}_H$ are found from the solution of Eqs. (6.35)–(6.37), the local electric and magnetic fields in the plane $z = -l_0 - d/2$ are given by the equations

$$\mathbf{E}_1 = \mathbf{E} + \frac{2\pi}{c}[\mathbf{n} \times \mathbf{j}_H] \qquad \mathbf{H}_1 = \mathbf{H} + \frac{2\pi}{c}[\mathbf{n} \times \mathbf{j}_E] \tag{6.38}$$

which follow from Eqs. (6.21) and (6.22) and definitions of the fields $\mathbf{E}$ and $\mathbf{H}$. Note that the field $\mathbf{E}_1(\mathbf{r})$ usually is measured in a typical near-field experiment (see Chapter 3). The effective parameters u_e and w_e are defined in a usual way

$$\langle\mathbf{j}_E\rangle = u_e\mathbf{E}_0 \equiv u_e(\langle\mathbf{E}_1\rangle + \langle\mathbf{E}_2\rangle)/2 \tag{6.39}$$
$$\langle\mathbf{j}_H\rangle = w_e\mathbf{H}_0 \equiv w_e(\langle\mathbf{H}_1\rangle + \langle\mathbf{H}_2\rangle)/2 \tag{6.40}$$

These expressions are substituted into Eqs. (6.21) and (6.22), which are averaged over the $\{x, y\}$ coordinates to obtain equations

$$[\mathbf{n} \times (\langle\mathbf{H}_2\rangle - \langle\mathbf{H}_1\rangle)] = \frac{2\pi}{c}u_e(\langle\mathbf{E}_1\rangle + \langle\mathbf{E}_2\rangle) \tag{6.41}$$

$$[\mathbf{n} \times (\langle\mathbf{E}_2\rangle - \langle\mathbf{E}_1\rangle)] = \frac{2\pi}{c}w_e(\langle\mathbf{H}_1\rangle + \langle\mathbf{H}_2\rangle) \tag{6.42}$$

for the averaged fields that determine the optical response of an inhomogeneous film.

Let us suppose that the wave enters the film from the right half-space (see Fig. 6.1), so that its amplitude is proportional to e^{-ikz}. The incident wave is partially reflected and partially transmitted through the film. The electric field amplitude in

the right half-space, away from the film, can be written as $\mathbf{e}[e^{-ikz} + re^{ikz}]$, where r is the reflection coefficient and $\mathbf{e}$ is the polarization vector. Then, the electric component of the EM wave well behind the film acquires the form $\mathbf{e}\ te^{-ikz}$, where t is the transmission coefficient. It is supposed for simplicity that the film has no optical activity, therefore wave polarization $\mathbf{e}$ remains the same before and after the film. At the planes $z = d/2 + l_0$ and $z = -d/2 - l_0$, the average electric field equals to $\langle\mathbf{E}_2\rangle$ and $\langle\mathbf{E}_1\rangle$, respectively. Now, the wave away from the film is matched by the average fields in the planes $z = d/2 + l_0$ and $z = -d/2 - l_0$, that is, $\langle\mathbf{E}_2\rangle = \mathbf{e}[e^{-ik(d/2+l_0)} + re^{ik(d/2+l_0)}]$ and $\langle\mathbf{E}_1\rangle = \mathbf{e}\ te^{ik(d/2+l_0)}$. The same matching, but with magnetic fields, gives $\langle\mathbf{H}_2\rangle = [\mathbf{n} \times \mathbf{e}][-e^{-ik(d/2+l_0)} + re^{ik(d/2+l_0)}]$ and $\langle\mathbf{H}_1\rangle = -[\mathbf{n} \times \mathbf{e}]te^{ik(d/2+l_0)}$ in the planes $z = d/2 + l_0$ and $z = -d/2 - l_0$, respectively. Substitution of these expressions for the fields $\langle\mathbf{E}_1\rangle$, $\langle\mathbf{E}_2\rangle$, $\langle\mathbf{H}_1\rangle$, and $\langle\mathbf{H}_2\rangle$ in Eqs. (6.41) and (6.42) gives two scalar, linear equations for reflection r and transmission t coefficients. Solution to these equations gives the reflectance and transmittance

$$R \equiv |r|^2 = \left|\frac{\frac{2\pi}{c}(u_e + w_e)}{\left(1 + \frac{2\pi}{c}u_e\right)\left(1 - \frac{2\pi}{c}w_e\right)}\right|^2 \tag{6.43}$$

$$T \equiv |t|^2 = \left|\frac{1 + \left(\frac{2\pi}{c}\right)^2 u_e w_e}{\left(1 + \frac{2\pi}{c}u_e\right)\left(1 - \frac{2\pi}{c}w_e\right)}\right|^2 \tag{6.44}$$

and absorbance

$$A = 1 - T - R \tag{6.45}$$

of the film. Therefore the effective Ohmic parameters u_e and w_e completely determine the optical properties of inhomogeneous films.

Thus the problem of the field distribution and optical properties of the metal–dielectric films reduces to uncoupled quasistatic conductivity problems Eqs. (6.35) and (6.36) to which extensive theory already exist. Thus numerous methods developed in the percolation theory can be used to find the effective parameters u_e and w_e of the film (see Section 6.4).

Now, let us consider the case of the strong skin effect in metal grains and trace the evolution of the optical properties of a semicontinuous metal film when the surface density p of metal is increasing. When $p = 0$, the film is purely dielectric and the effective parameters u_e and w_e coincide with the dielectric Ohmic parameters given by Eq. (6.33). By substituting $u_e = u_d$ and $w_e = w_d$ into Eqs. (6.43)–(6.45) and assuming that the dielectric film has no losses and is optically thin ($dk\varepsilon_d \ll 1$), we obtain the reflectance $R = d^2(\varepsilon_d - 1)^2k^2/4$, transmittance $T = 1 - d^2(\varepsilon_d - 1)^2k^2/4$,

and the absorbance $A = 0$ that coincides with the well-known results for a thin dielectric film [48,49].

It is not surprising that a film without losses has zero absorbance. The losses are also absent in the limit of full coverage, when the metal concentration $p = 1$, since the strong skin effect is considered when penetration length (skin depth) $\delta = 1/k \operatorname{Im} n_m$ is negligible in comparison with the film thickness d. In this case, the film is a perfect metal mirror. Indeed, by substituting the Ohmic parameters $u_e = u_m$ and $w_e = w_m$ from Eq. (6.32) into Eqs. (6.43)–(6.45) we obtain for the reflectance $R = 1$, while the transmittance T and absorbance A are both equal to zero. Note that the optical properties of the film do not depend on the particle size D for the metal concentration $p = 0$ and $p = 1$, since properties of the dielectric and continuous metal films do not depend on the shape of the metal grains.

Now, we consider the film at the percolation threshold $p = p_c$ with $p_c = \frac{1}{2}$ for a self-dual system [3,4]. A semicontinuous metal film may be thought of as a mirror, which is broken into small pieces with typical size D much smaller than the wavelength λ. At the percolation threshold, the exact Dykhne formulas $u_e = \sqrt{u_d u_m}$ and $w_e = \sqrt{w_d w_m}$ hold [50]. Thus the following equations for the effective Ohmic parameters are obtained from Eqs. (6.33) and (6.32)

$$\frac{2\pi}{c}\, u_e(p_c) = \sqrt{\varepsilon'_d} \qquad \frac{2\pi}{c}\, w_e(p_c) = i\,\frac{Dk}{4}\,\sqrt{1+\frac{2d}{D}} \tag{6.46}$$

From these equations it follows that $|w_e/u_e| \sim Dk \ll 1$ and the effective Ohmic parameter w_e can be neglected in comparison with u_e. By substituting the effective Ohmic parameter $u_e(p_c)$ given by Eq. (6.46) in Eqs. (6.43)–(6.45), the optical properties at the percolation are obtained

$$R(p_c) = \frac{\varepsilon'_d}{(1+\sqrt{\varepsilon'_d})^2} \tag{6.47}$$

$$T(p_c) = \frac{1}{(1+\sqrt{\varepsilon'_d})^2} \tag{6.48}$$

$$A(p_c) = \frac{2\sqrt{\varepsilon'_d}}{(1+\sqrt{\varepsilon'_d})^2} \tag{6.49}$$

Remember that reduced dielectric function $\varepsilon'_d = 1 + 2\varepsilon_d d/D$. When metal grains are oblate enough so that $\varepsilon_d d/D \ll 1$ and $\varepsilon'_d \to 1$, the above expressions simplify to the universal result

$$R = T = \tfrac{1}{4} \qquad A = \tfrac{1}{2} \tag{6.50}$$

Thus, there is effective adsorption in semicontinuous metal films even for the case when neither dielectric nor metal grains absorb light energy. The mirror broken into small pieces effectively absorbs energy from the EM field. The effective

absorption in a loss-free film means that the EM energy is stored in the system and that the amplitudes of the local EM field increase up to infinity. In any real semicontinuous metal film, the local field saturates due to nonzero losses, but significant field fluctuations take place over the film when losses are small, as discussed below.

To find the optical properties of semicontinuous films for arbitrary metal concentration p, the effective medium theory can be implemented, which was originally developed to provide a semiquantitative description of the transport properties of percolating composites [3]. The effective medium theory, when being applied to Eqs. (6.35), (6.39), (6.36), and (6.40), results in the following equations for the effective parameters:

$$u_e^2 - \Delta p u_e(u_m - u_d) - u_d u_m = 0 \tag{6.51}$$

$$w_e^2 - \Delta p w_e(w_m - w_d) - w_d w_m = 0 \tag{6.52}$$

where the reduced concentration $\Delta p = (p - p_c)/p_c$, $\left(p_c = \frac{1}{2}\right)$ is introduced. It follows from Eq. (6.52) that for the considered case of a strong skin effect, when the Ohmic parameters w_m and w_d are given by Eqs. (6.32) and (6.33), the effective Ohmic parameter $|w_e| \ll c$ for all metal concentrations p. Therefore, the parameter w_e is negligible in Eqs. (6.43) and (6.44). For further simplification, the Ohmic parameter u_d can be neglected in comparison with u_m in the second term of Eq. (6.51) [cf. Eqs. (6.32) and (6.33)]. Then, introduction of the dimensionless Ohmic parameter $u'_e = (2\pi/c)u_e$ allows us to rewrite Eq. (6.51) as

$$u_e'^2 - 2i\,\frac{\lambda \Delta p}{\pi D}\,u'_e - \varepsilon'_d = 0 \tag{6.53}$$

Right at the percolation threshold $p = p_c = \frac{1}{2}$, when the reduced concentration $\Delta p = 0$, Eq. (6.53) gives the effective Ohmic parameter $u'_e(p_c) = \sqrt{\varepsilon'_d}$, which coincides exactly with Eq. (6.46) and results in reflectance, transmittance, and absorbance given by Eqs. (6.47)–(6.49), respectively. For concentrations different than the percolation threshold, Eq. (6.53) gives

$$u'_e = i\,\frac{\lambda \Delta p}{\pi D} + \sqrt{-\left(\frac{\lambda \Delta p}{\pi D}\right)^2 + \varepsilon'_d} \tag{6.54}$$

which becomes purely imaginary for $|\Delta p| > \pi D\sqrt{\varepsilon'_d}/\lambda$. Then, Eqs. (6.47)–(6.49) result in zero absorbance, $A = 1 - R - T = 1 - |u'_e|^2/|1 + u'_e|^2 - 1/|1 + u'_e|^2 = 0$ (recall that the effective Ohmic parameter w_e is neglected). In the vicinity of a percolation threshold, namely, for

$$|\Delta p| < \frac{\pi D}{\lambda}\,\sqrt{\varepsilon'_d} \tag{6.55}$$

the effective Ohmic parameter u'_e has a nonvanishing real part and, therefore, the absorbance

$$A = \frac{2\sqrt{-(\lambda\Delta p/\pi D)^2 + \varepsilon'_d}}{1 + \varepsilon'_d + 2\sqrt{-(\lambda\Delta p/\pi D)^2 + \varepsilon'_d}} \tag{6.56}$$

is nonzero and has a well-defined maximum at the percolation threshold; the width of the maximum is inversely proportional to the wavelength. The effective absorption in almost loss-free semicontinuous metal film means that local EM fields strongly fluctuate in the system, as was speculated above. The spectral width for the strong fluctuations should be the same as the width of the absorption maximum, that is, it is given by Eq. (6.55).

Note that the effective parameters u_e and w_e can be determined experimentally by measuring the amplitude and phase of the transmitted and reflected waves using, for example, a waveguide technique (see, [51] and references cited therein), or by measuring the film reflectance as a function of the fields $\mathbf{E}_1$ and $\mathbf{H}_1$. In this case, a metal screen placed behind the film can be used to control the values of these fields [52,53].

6.4. COMPUTER SIMULATIONS OF LOCAL ELECTRIC AND MAGNETIC FIELDS

6.4.1. Kirchhoff's Equations

To find the local electric $\mathbf{E}(\mathbf{r})$ and magnetic $\mathbf{H}(\mathbf{r})$ fields, Eqs. (6.35) and (6.36) should be solved. First, consider Eq. (6.35), which is convenient to rewrite in terms of the dimensionless "dielectric constant"

$$\tilde{\varepsilon} = 4\pi i u(\mathbf{r})/\omega d \tag{6.57}$$

as follows:

$$\nabla \cdot [\tilde{\varepsilon}(\mathbf{r})\nabla\phi(\mathbf{r})] = \mathcal{E} \tag{6.58}$$

where $\phi(\mathbf{r})$ is the fluctuating part of the potential $\phi'(\mathbf{r})$ so that $\nabla\phi'(\mathbf{r}) = \nabla\phi(\mathbf{r}) - \mathbf{E}_0$, $\langle\phi(\mathbf{r})\rangle = 0$, and $\mathcal{E} = \nabla \cdot [\tilde{\varepsilon}(\mathbf{r})\mathbf{E}_0]$. Remember that the "external" field $\mathbf{E}_0$ is defined by Eq. (6.37). For the metal–dielectric films considered here, local dielectric constant $\tilde{\varepsilon}(\mathbf{r})$ equals $\tilde{\varepsilon}_m = 4\pi i u_m/\omega d$ and $\tilde{\varepsilon}_d = \varepsilon'_d D/2d$ for the metal and dielectric regions, respectively. The external field $\mathbf{E}_0$ in Eq. (6.58) can be chosen real, while the local potential $\phi(\mathbf{r})$ takes complex values since the metal dielectric constant $\tilde{\varepsilon}_m$ is complex $\tilde{\varepsilon}_m = \tilde{\varepsilon}'_m + i\tilde{\varepsilon}''_m$. In the quasistatic limit, when the skin depth δ is much

larger than the film thickness d, the dielectric constant $\tilde{\varepsilon}_m$ coincides with the metal dielectric constant ε_m as it follows from Eq. (6.31).

To get insight into the high-frequency properties of metals, a simple model known as a Drude metal is considered, which semiquantitaively reproduces the basic optical properties of a metal [54]. In this approach, the dielectric constant of metal grains can be approximated by the Drude formula

$$\varepsilon_m(\omega) = \varepsilon_b - (\omega_p/\omega)^2/(1 + i\omega_\tau/\omega) \tag{6.59}$$

where ε_b is contribution to ε_m due to the interband transitions: ω_p is the plasma frequency, and $\omega_\tau = 1/\tau \ll \omega_p$ is the relaxation rate. In the high-frequency range considered here, losses in metal grains are relatively small, $\omega_\tau \ll \omega$. Therefore, the real part ε'_m of the metal dielectric function ε_m is much larger (in modulus) than the imaginary part ε''_m ($|\varepsilon'_m|/\varepsilon''_m \cong \omega/\omega_\tau \gg 1$), and ε'_m is negative for the frequencies ω less than the renormalized plasma frequency,

$$\tilde{\omega}_p = \omega_p/\sqrt{\varepsilon_b} \tag{6.60}$$

Thus, the metal conductivity $\sigma_m = -i\omega\varepsilon_m/4\pi \cong (\varepsilon_b\tilde{\omega}_p^2/4\pi\omega)[i(1 - \omega^2/\tilde{\omega}_p^2) + \omega_\tau/\omega]$ is characterized by the dominant imaginary part for $\tilde{\omega}_p > \omega \gg \omega_\tau$, that is, it is of inductive character. The same is true for the Ohmic parameter u_m in the quasistatic limit since it is just proportional to the metal conductivity in this limit. In the opposite case of the strong skin effect, the Ohmic parameter u_m is inductive according to Eq. (6.32) for all spectral ranges regardless of the metal properties. Therefore, the metal grains can be modeled as inductances L while the dielectric gaps can be represented by capacitances C. This model works for the optic and IR regardless of the metal grain size and holds for *all* spectral ranges when the skin effect is strong in the metal grains. Then, the percolation metal–dielectric film represents a set of randomly distributed L and C elements. The collective surface plasmons excited by the external field, can be thought of as resonances in different $L - C$ circuits, and the excited surface plasmon eigenstates are seen as giant fluctuations of the local field [50].

Note that Ohmic parameter w takes the same sign and rather close absolute values for metal and dielectric grains according to Eqs. (6.31)–(6.33). A film can be thought of as a collection of C elements in "w" space. Therefore the resonance phenomena are absent in a solution of Eq. (6.36). The fluctuations of the potential ψ' can be indeed neglected in comparison to the φ' fluctuations. For this reason, we concentrate attention on the properties of the "electric" field $\mathbf{E}(\mathbf{r}) = -\nabla\phi'(\mathbf{r}) = -\nabla\phi(\mathbf{r}) + \mathbf{E}_0$ that can be found from solution of Eq. (6.58).

Because of difficulties in finding a solution to the Poisson Eq. (6.35) or (6.58), a great deal of use is made of the tight binding model in which metal and dielectric particles are represented by metal and dielectric bonds of a square lattice. After such discretization, Eq. (6.58) acquires the form of the Kirchhoff's equations defined on a square lattice [3]. The Kirchhoff's equations can be written in terms of the local

dielectric constant and it is assumed that the external electric field $\mathbf{E}_0$ is directed along the "x" axis. Thus, the following set of equations are obtained

$$\sum_j \tilde{\varepsilon}_{ij}(\phi_j - \phi_i) = \sum_j \tilde{\varepsilon}_{ij} E_{ij} \tag{6.61}$$

where ϕ_i and ϕ_j are the electric potentials determined at the sites of the square lattice and the summation is over the nearest neighbors of the site i. The electromotive force (emf) E_{ij} takes the value $E_0 a_0$ for the bond $\langle ij \rangle$ in the positive x direction (where a_0 is the spatial period of the square lattice) and $-E_0 a_0$, for the bond $\langle ij \rangle$ in the $-x$ direction; $E_{kj} = 0$ for the other four bonds at the site i. Thus the composite is modeled by a capacitor–inductor–resistor network represented by Kirchhoff's equations (6.61). The emf forces E_{ij} represent the external electric field applied to the system. In transition from the continuous medium described by Eq. (6.58) to the random network described by Eq. (6.61), it is usually supposed [1–4] that bond permittivities $\tilde{\varepsilon}_{ij}$ are statistically independent and a_0 is set to be equal to the metal grain size, $a_0 = a$. In the considered case of a two component metal–dielectric random film, the permittivities $\tilde{\varepsilon}_{ij}$ take the values $\tilde{\varepsilon}_m$ and $\tilde{\varepsilon}_d$, with probabilities p and $1 - p$, respectively. The assumption that the bond permittivities $\tilde{\varepsilon}_{ij}$ in Eq. (6.61) are statistically independent considerably simplify computer simulations as well as analytical consideration of local optical fields in the film. Note that important critical properties are universal, that is, they are independent of details of a model (e.g., possible correlation of permittivities $\tilde{\varepsilon}_{ij}$ in different bonds).

6.4.2. Numerical Model

Now, there exist very efficient numerical methods for calculating the effective conductivity of composite materials (see [1–4,8,55,56]), but they typically do not allow calculations of the field distributions. To calculate local field distribution, a new original method had been developed. It is based on the real-space renormalization group (RSRG) method that was suggested for percolation by Reynolds, et al. [57] and Sarychev [58], and then extended to study the conductivity [59] and the permeability of oil reservoirs [60]. By following the approach used by Aharony, the RSRG method was adopted to finding the field distributions in the following way [38,39,61]. First, a square lattice of L-R (metal) and C (dielectric) bonds was generated using a random number generator. As seen in Fig. 6.3, such a lattice can be considered as a set of "corner" elements. One of such elements is labeled as (ABCDEFGH) in Fig. 6.3. In the first stage of the RSRG procedure, each of these elements is replaced by the two Wheatstone bridges, as shown in Fig. 6.3. After this transformation, the initial square lattice is converted to another square lattice, with the distance between the sites twice larger and with each bond between the two nearest-neighboring sites being the Wheatstone bridge. Note that there is a 1:1 correspondence between the x bonds in the initial lattice and the x bonds in the x directed bridges of the transformed lattice, as seen in Fig. 6.3. The same 1:1 correspondence also exists between the y bonds. The transformed lattice is also a

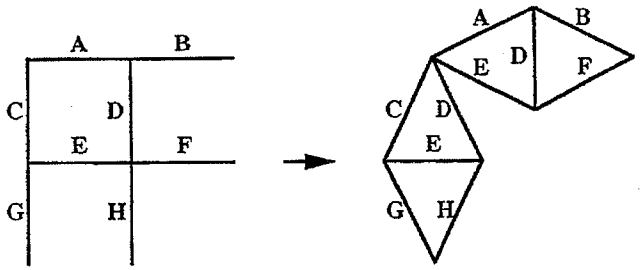

Figure 6.3. The real-space renormalization scheme.

square lattice, and we can again apply to it the RSRG transformation. We continue this procedure until the size $\mathcal{L}$ of the system is reached. As a result, instead of the initial lattice we have two large Wheatstone bridges in the x and y directions. Each of them has a hierarchical structure consisting of bridges with the sizes from 2 to $\mathcal{L}$. Because the 1:1 correspondence is preserved at each step of the transformation, the correspondence also exists between the elementary bonds of the transformed lattice and the bonds of the initial lattice. After using the RSRG transformation, the periodic boundary conditions (see, e.g., [8]) are applied and the Kirchhoff's equations (6.61) are solved to determine the fields and the currents in all the bonds of the transformed lattice. Due to the hierarchical structure of the transformed lattice, these equations can be solved exactly. Then, the 1:1 correspondence between the elementary bonds of the transformed lattice and the bonds of the initial square lattice is used to find the field distributions in the initial lattice as well as its effective dielectric constant. The number of operations to get the full distributions of the local fields is proportional to $\mathcal{L}^2$ and is much less than the $\mathcal{L}^7$ operations needed in the transform-matrix method [3,62] and the $\mathcal{L}^3$ operations needed in the well-known Frank–Lobb algorithm [55], which does not provide the field distributions but the effective conductivity only. The RSRG procedure is certainly not exact since the effective connectivity of the transformed system does not repeat the connectivity of the initial square lattice exactly. To check the accuracy of the RSRG, the $2d$ percolation problem was solved using this method [39]. Namely, the effective parameters were calculated for a two-component composite with the real metallic conductivity σ_m much larger than the real conductivity σ_d of the dielectric component $\sigma_m \gg \sigma_d$. It obtained the percolation threshold $p_c = 0.5$ and the effective conductivity at the percolation threshold that is very close to $\sigma(p_c) = \sqrt{\sigma_m \sigma_d}$. These results coincide with the exact ones for $2d$ composites [50]. This is not surprising since the RSRG procedure preserves the self-duality of the initial system. The critical exponents obtained by the RSRG are also in agreement with known values of the exponents from the percolation theory [1,3]. Thus the ratio of the critical exponent s for the static dielectric constant and the exponent ν for the percolation correlation length is equal to $s/\nu \simeq 0.94$, the ratio of the critical exponent t for the static conductivity and the exponent ν is equal to $t/\nu \simeq 0.82$. These results should be compared with $s/\nu \simeq t/\nu \simeq 1$ that follow from the percolation theory for $2d$ composites. Therefore, there are good reasons to believe that the

numerical method describes at least qualitatively the field distributions on semicontinuous metal films. Below the RSRG exponents $s/\nu \simeq 0.94$ and $t/\nu \simeq 0.8$ are used when the computer results obtained by RSRG are compared with the scaling theory.

6.4.3. Giant Fluctuations of the Local Fields

The real-space renormalization method described above was employed to solve Eq. (6.61) and to calculate the potentials ϕ_i in the lattice. Then, we find the local field $\mathbf{E}(\mathbf{r})$ and electric current $\mathbf{j}_E(\mathbf{r})$ in terms of the average field $\mathbf{E}_0$. The effective Ohmic parameter u_e is determined by Eq. (6.39), which can be written as $\langle \mathbf{j}_E \rangle = u_e \mathbf{E}_0$. The effective dielectric constant $\tilde{\varepsilon}_e$ is equal to $4\pi i u_e/\omega d$. In the same manner, the field $\mathbf{H}(\mathbf{r})$, the magnetic current $\mathbf{j}_H(\mathbf{r})$, and the effective parameter w_e can be found from Eq. (6.36) and its lattice discretization. Note that the *same* lattice should be used to determined the fields $\mathbf{E}(\mathbf{r})$ and $\mathbf{H}(\mathbf{r})$. The directions of the external fields $\mathbf{E}_0$ and $\mathbf{H}_0$ may be chosen arbitraryly when the effective parameters u_e and w_e are calculated since the effective parameters do not depend on the direction of the field for a film, which is isotropic as a whole.

Though the effective parameters do not depend on the external field, the local electric $\mathbf{E}_1(\mathbf{r})$ and magnetic and $\mathbf{H}_1(\mathbf{r})$ fields do depend on the incident wave. The local fields $\mathbf{E}_1(\mathbf{r})$ and $\mathbf{H}_1(\mathbf{r})$ are define in the reference plane $z = -d/2 - l_0$ (see Fig. 6.1). Note that the field $\mathbf{E}_1(\mathbf{r})$ is observed in a typical near-field experiment (see Chapter 3). For the calculations below the electric and magnetic fields of the incident EM wave have been chosen in the form $\langle \mathbf{E}_1 \rangle = \{1, 0, 0\}$ and $\langle \mathbf{H}_1 \rangle = \{0, -1, 0\}$ in the plane $z = -l_0 - d/2$. This choice corresponds to the wavevector of the incident wave as $\mathbf{k} = (0, 0, -k)$, that is, there is only a transmitted wave behind the film (see Fig. 6.1). It follows from the average of Eq. (6.38), which can be written as $\langle \mathbf{E}_1 \rangle = \mathbf{E}_0 + (2\pi/c) w_e [\mathbf{n} \times \mathbf{H}_0]$ and $\langle \mathbf{H}_1 \rangle = \mathbf{H}_0 + (2\pi/c) u_e [\mathbf{n} \times \mathbf{E}_0]$ that the fields $\mathbf{E}_0$ and $\mathbf{H}_0$ are given by

$$\mathbf{E}_0 = \frac{\langle \mathbf{E}_1 \rangle - (2\pi/c) w_e [\mathbf{n} \times \langle \mathbf{H}_1 \rangle]}{1 + (2\pi/c)^2 u_e w_e} \qquad \mathbf{H}_0 = \frac{\langle \mathbf{H}_1 \rangle - (2\pi/c) u_e [\mathbf{n} \times \langle \mathbf{E}_1 \rangle]}{1 + (2\pi/c)^2 u_e w_e}. \quad (6.62)$$

These values of the fields $\mathbf{E}_0$ and $\mathbf{H}_0$ are used to calculate the local fields $\mathbf{E}(\mathbf{r})$ and $\mathbf{H}(\mathbf{r})$. The local electric $\mathbf{E}_1(\mathbf{r})$ and magnetic $\mathbf{H}_1(\mathbf{r})$ fields are restored then from the fields $\mathbf{E}(\mathbf{r})$ and $\mathbf{H}(\mathbf{r})$ by using Eq. (6.38).

The local electric and magnetic fields have been calculated in silver-on-glass semicontinuous film as functions of the surface concentration p of silver grains. The typical glass dielectric constant ε_d is $\varepsilon_d = 2.2$. The dielectric function for silver was chosen in the Drude form (6.59); the following parameters were also used in Eq. (6.59): the interband-transition contribution $\varepsilon_b = 5$, the plasma frequency $\omega_p = 9.1$ eV, and the relaxation frequency $\omega_\tau = 0.021$ eV [63]. The metal grains are supposed to be oblate. The ratio of the grain thickness d (film thickness) and the grain diameter D has been chosen as $D/d = 3$, the same as used in [18]. To consider the skin effect of different strengths (i.e., different interactions between the electric

and magnetic fields), we vary the size d of silver particles in a wide range, $d = 1 \div 100$ nm. The size of metal grains in semicontinuous metal films is usually on the order of a few nanometers, but it can be increased significantly by using the proper method of preparation [64]. For microwave experiments [20] the films were prepared by the lithography method, so that the size of the metal particle could vary over a large range.

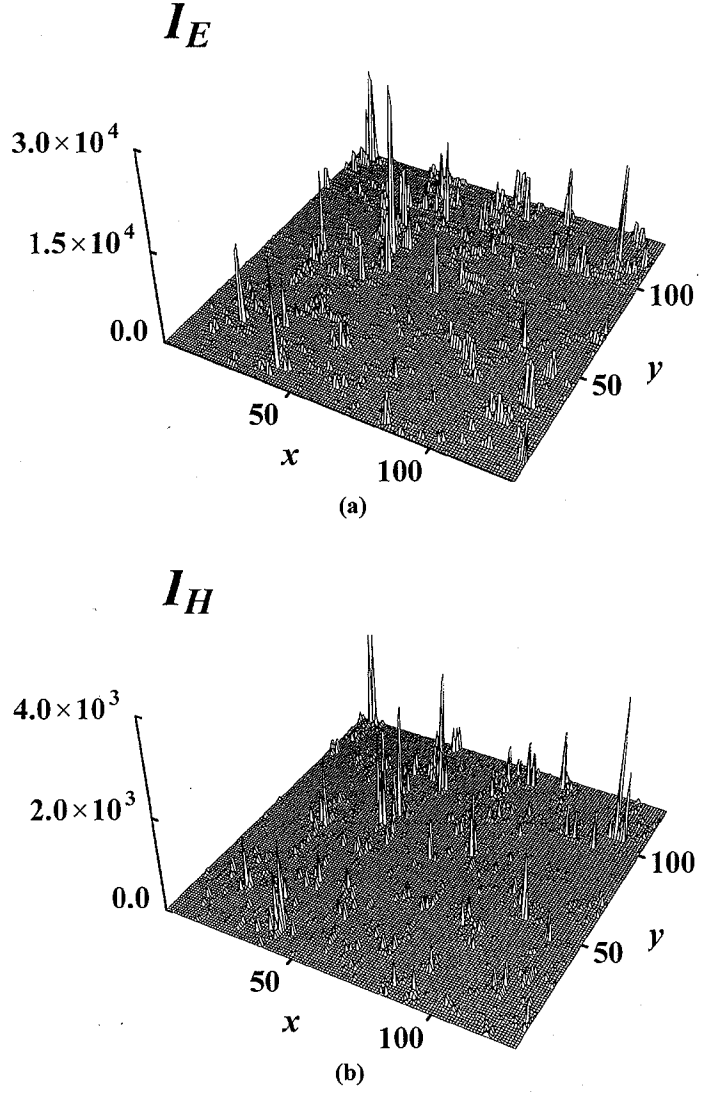

Figure 6.4. Distribution of local EM field intensities (a) $I_E = |\mathbf{E}_1(\mathbf{r})|^2/|\langle \mathbf{E}_1 \rangle|^2$ and (b) $I_H = |\mathbf{H}_1(\mathbf{r})|^2/|\langle \mathbf{H}_1 \rangle|^2$ in a semicontinuous silver film at the percolation threshold for $\lambda = 1\mu$m and $\delta/d = 4.5$, where δ is the skin depth and d is the thickness of the film.

The space distribution of the electric and magnetic fields was calculated at two sets of parameters, as illustrated in Figs. 6.4–6.7. In Figs. 6.4 and 6.5, we show the electric and magnetic field distributions for $\lambda = 1\,\mu$m and two different thicknesses d of the film, $d = 5$ and $d = 50$ nm. The first thickness (Fig. 6.4) corresponds to a weak skin effect since the dimensionless thickness is small, $\Delta \equiv d/\delta = 0.2$, where $\delta = 1/k\,(\mathrm{Im}\, n_m)$ is the skin depth. In this case, we observe the giant field fluctuations of the local electric field; the magnetic field also strongly fluctuates over the film but the field peaks are small compared to the electric field. The reason is that the film itself is not magnetic, $\mu_d = \mu_m = 1$, and the interaction of the magnetic field with the electric field through the skin effect is relatively small.

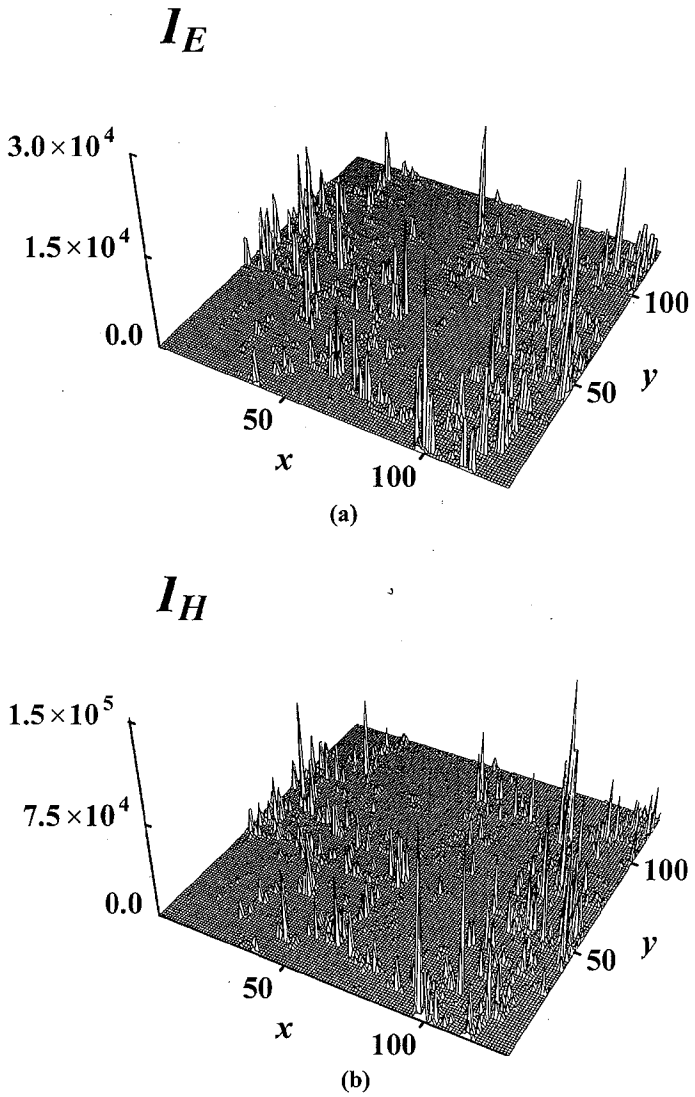

Figure 6.5. Distribution of local EM field intensities (a) $I_E = |\mathbf{E}_1(\mathbf{r})|^2/|\langle\mathbf{E}_1\rangle|^2$ and (b) $I_H = |\mathbf{H}_1(\mathbf{r})|^2/|\langle\mathbf{H}_1\rangle|^2$ in a semicontinuous silver film at the percolation threshold for $\lambda = 1\,\mu$m and $\delta/d = 0.45$.

In Fig. 6.5, we show results for a significant skin effect, when the film thickness $d = 50$ nm and the dimensionless thickness exceeds 1, $\Delta = 2.2$. It is interesting to

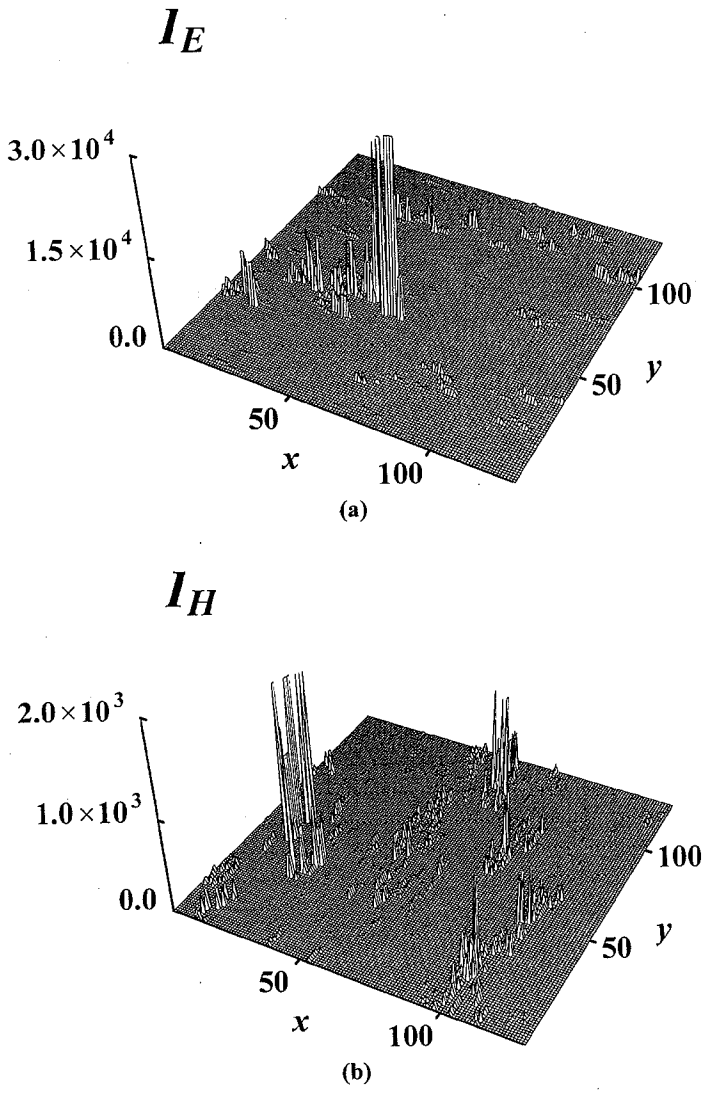

Figure 6.6. Distribution of local EM field intensities (a) $I_E = |\mathbf{E}_1(\mathbf{r})|^2/|\langle\mathbf{E}_1\rangle|^2$ and (b) $I_H = |\mathbf{H}_1(\mathbf{r})|^2/|\langle\mathbf{H}_1\rangle|^2$ in a semicontinuous silver film at the percolation threshold for $\lambda = 10\,\mu$m and $\delta/d = 4.5$.

note that the amplitude of the electric field is roughly the same as in Fig. 6.4(a), despite the fact that the parameter Δ increased by one order of magnitude. In contrast, the local magnetic field (Fig. 6.5(b)) is strongly increased in this case so that the amplitude of the magnetic field in peaks is of the same order of magnitude as the electric field maxima. This behavior can be understood by considering the spatial moments of the local magnetic field as shown in Section 6.5.

In Figs. 6.6 and 6.7, we show results of the calculations for the local electric and magnetic fields at $\lambda = 10\,\mu$m, when the metal dielectric constant $|\varepsilon_m| \sim 10^4$. We see

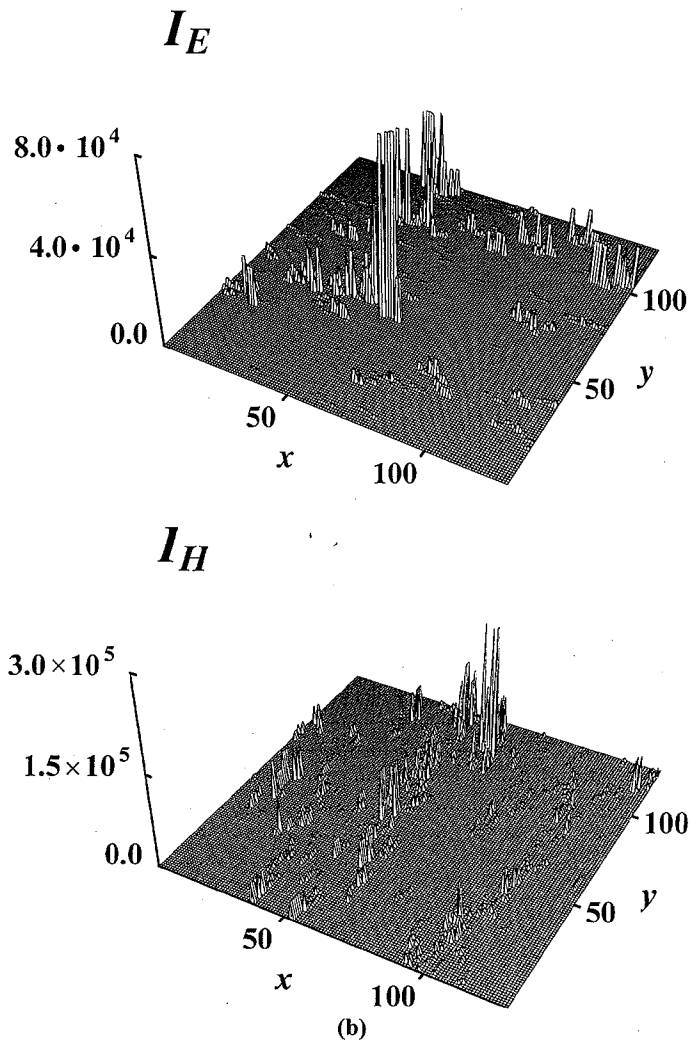

Figure 6.7. Distribution of local EM field intensities (a) $I_E = |\mathbf{E}_1(\mathbf{r})|^2/|\langle \mathbf{E}_1 \rangle|^2$ and (b) $I_H = |\mathbf{H}_1(\mathbf{r})|^2/|\langle \mathbf{H}_1 \rangle|^2$ in a semicontinuous silver film at the percolation threshold for $\lambda = 10\,\mu$m and $\delta/d = 0.45$.

that in this case the local magnetic field can even exceed the electric field. Systematic computer simulation of the local electric field for a different wavelength and metal concentration a reader can find in [39,41–45]. The giant local field fluctuations were observe first in the microwave experiment [20] and then in the optic near-field experiments [21,22].

Being given the local fields, the effective parameters u_e and w_e can be found as well as the effective optical properties of the film. In Figs. 6.8 and 6.9, we show the

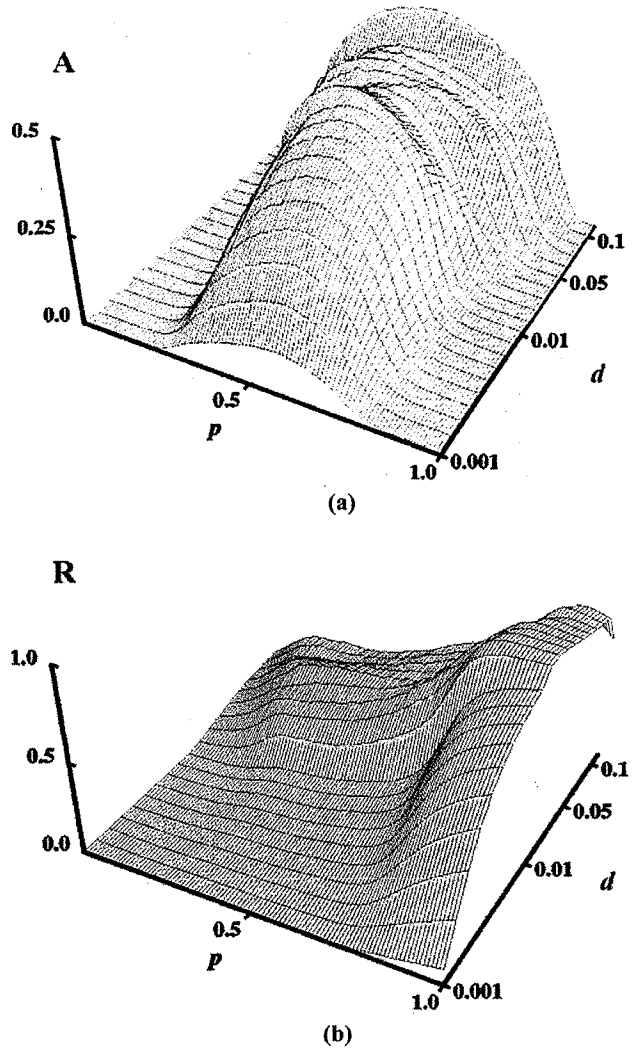

Figure 6.8. Computer simulation of (a) absorptance A, (b) reflectance R, and (c) transmittance T for a silver-on-glass semicontinous film as functions of metal concentration p and film thickness d (μm) at $\lambda = 1\,\mu$m.

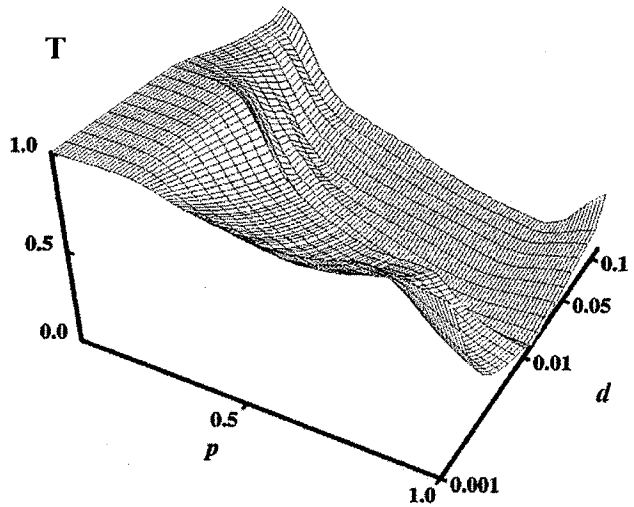

(c)

Figure 6.8. (*Continued*)

reflectance, transmittance, and absorbance as functions of silver concentration p, for wavelengths $\lambda = 1$ and $10\,\mu$m, respectively. The absorbance in these figures has an anomalous maximum in the vicinity of the percolation threshold that corresponds to the behavior predicted by Eq. (6.56). This maximum was first detected in the experiments [13–16]. The maximum in the absorption corresponds to strong fluctuations of the local fields. In Eq. (6.55), we have estimated the concentration range Δp

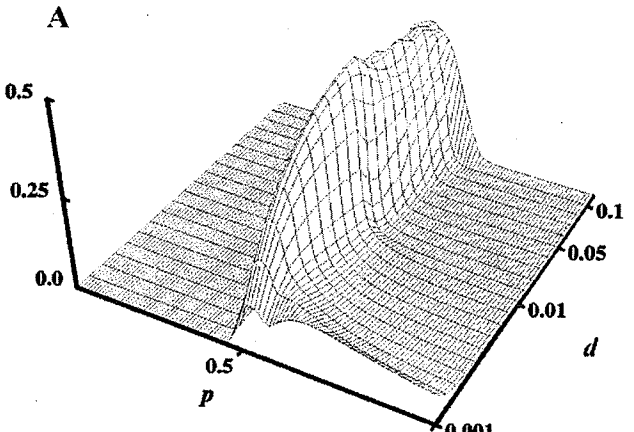

(a)

Figure 6.9. Computer simulation of (a) absorptance A, (b) reflectance R, and (c) transmittance T for a silver-on-glass semicontinous film as functions of metal concentration p and film thickness $d\,(\mu\text{m})$ at $\lambda = 10\,\mu$m.

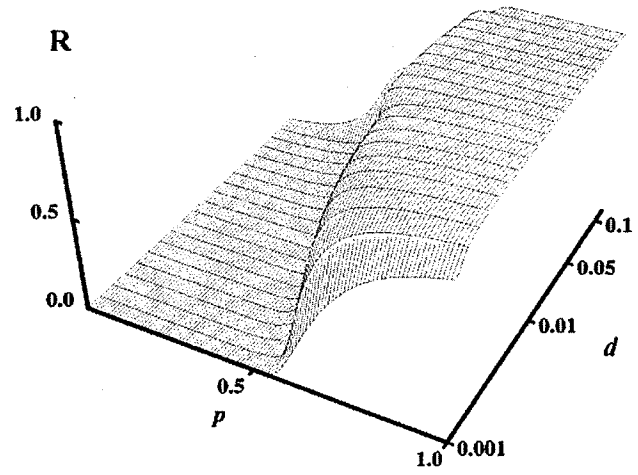

(b)

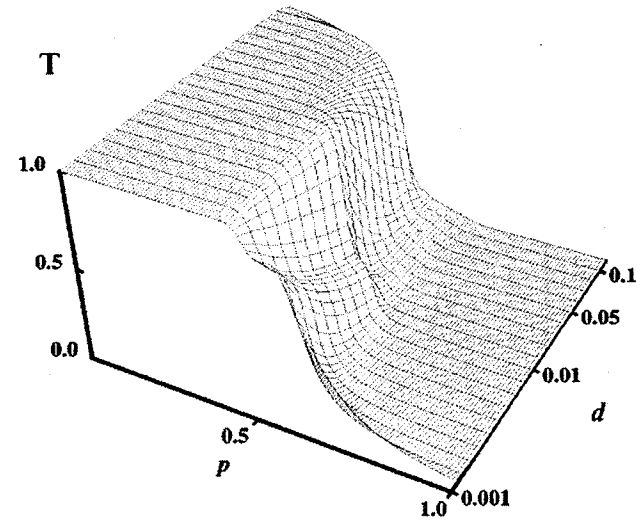

(c)

Figure 6.9. (*Continued*)

centered at the percolation threshold p_c (where the giant local field fluctuations occur) as $\Delta p \propto 1/\lambda$. Indeed, the absorbance shrinks at transition from Fig. 6.8 to Fig. 6.9, when the wavelength λ increases 10 times. In Figs. 6.10 and 6.11, we compare results of numerical simulations for the optical properties of silver semicontinuous films with calculations based on the effective medium approach [Eqs. (6.51) and (6.52)] represented in terms of the new Ohm's parameters u and v. Results of such a "dynamic" effective-medium theory are in good agreement with our numerical simulations for arbitrary skin effects.

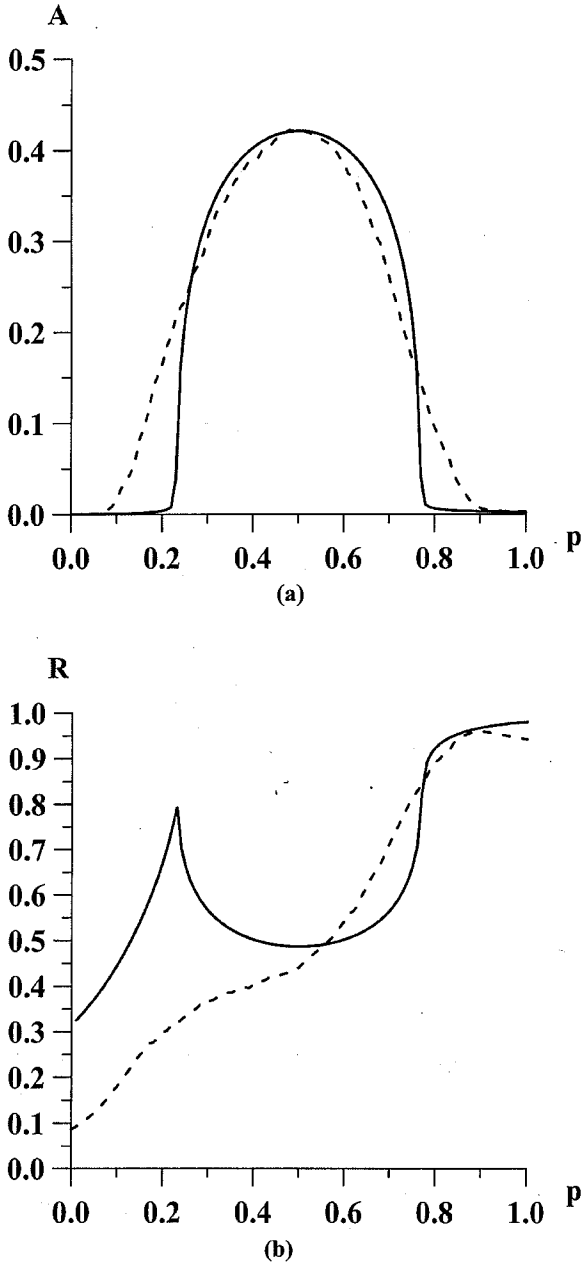

Figure 6.10. Results of computer simulations (dashed line) and the dynamic effective–medium theory (solid line) for (a) absorptance A, (b) reflectance R, and (c) transmittance T of a silver-on-glass semicontinuous film as a function of the metal concentration p at wavelengths $\lambda = 1\,\mu\text{m}$ and thickness $d = 50\,\text{nm}$.

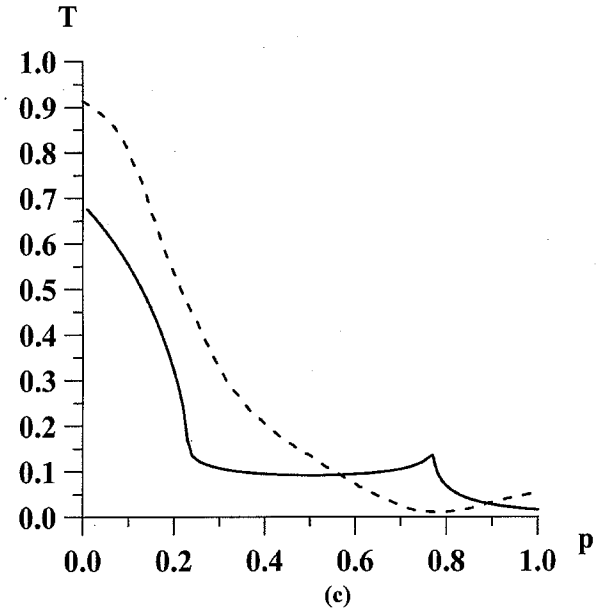

Figure 6.10. (*Continued*)

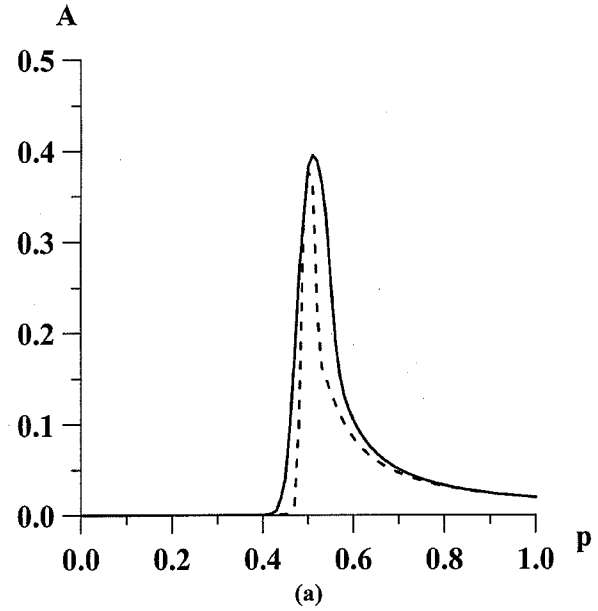

Figure 6.11. Results of computer simulations (dashed line) and the dynamic effective-medium theory (solid line) for (a) absorptance A, (b) reflectance R, and (c) transmittance T of a silver-on-glass semicontinuous film as a function of the metal concentration p at wavelengths $\lambda = 10\,\mu\text{m}$ and thickness $d = 5\,\text{nm}$.

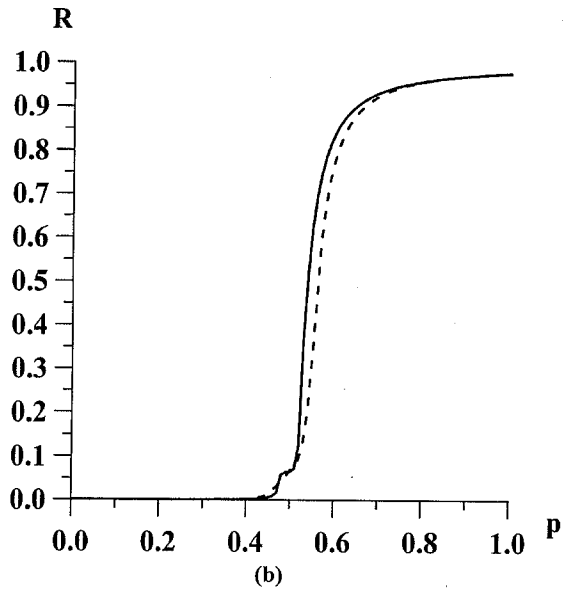

(b)

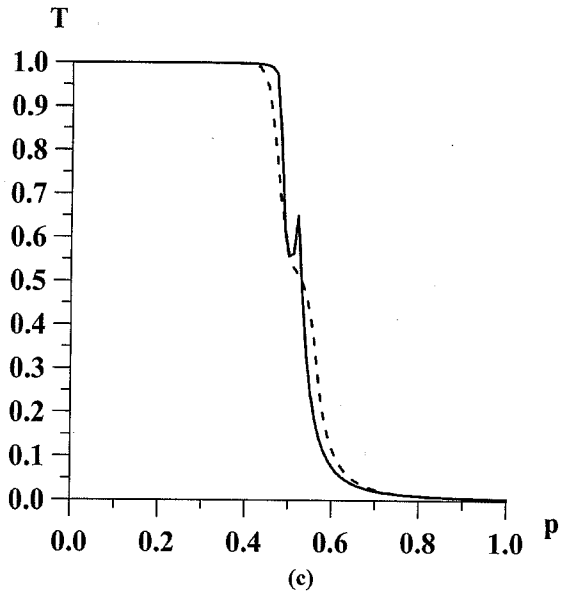

(c)

Figure 6.11. (*Continued*)

6.5. ANDERSON LOCALIZATION OF SURFACE PLASMONS

In this section, we follow the approach developed in recent papers [21,45,46]. To estimate the local field distribution analytically it is convenient to start with Kirchhoff's equations (6.61). For further consideration, it is assumed that the square lattice has a very large but finite number of sites N and rewrite Eq. (6.61) in matrix form with the "Hamiltonian" $\mathcal{H}$ defined in terms of the local dielectric constants,

$$\mathcal{H}\phi = \mathcal{E} \tag{6.63}$$

where ϕ is a vector of the local potentials $\phi = \{\phi_1, \phi_2, \ldots, \phi_N\}$ determined in all N sites of the lattice, vector $\mathcal{E}$ equals to $\mathcal{E}_i = \sum_j \tilde{\varepsilon}_{ij} E_{ij}$, as it follows from Eq. (6.61). The Hamiltonian $\mathcal{H}$ is $N \times N$ matrix that has off-diagonal elements $H_{ij} = -\tilde{\varepsilon}_{ij}$ and diagonal elements defined as $H_{ii} = \sum_j \tilde{\varepsilon}_{ij}$, where j refers to nearest neighbors of site i. The off-diagonal elements H_{ij} take values $\tilde{\varepsilon}_d > 0$ and $\tilde{\varepsilon}_m$, with probability p and $1 - p$, respectively. The diagonal elements H_{ii} are Eq. (6.61) distributed between $2d\tilde{\varepsilon}_m$ and $2d\tilde{\varepsilon}_d$, where d is the dimensionality of the space ($2d$ is the number of the nearest neighbors in d dimensional square lattice).

The dielectric constant $\tilde{\varepsilon}_m$ is negative in the visible and IR spectral ranges for a typical metal as it was discussed after Eq. (6.59). Therefore, $\tilde{\varepsilon}_m$ can be written as $\tilde{\varepsilon}_m = |\tilde{\varepsilon}'_m|(-1 + i\kappa)$, where the loss factor $\kappa = \tilde{\varepsilon}''_m/|\tilde{\varepsilon}'_m|$ is small, $\kappa \ll 1$. This equation for $\tilde{\varepsilon}_m$ holds in all spectral ranges if the skin effect is strong in the metal grains. It is shown below that the fluctuations of the local fields are significant when $\tilde{\varepsilon}'_m$ is negative and the losses are small. It is supposed in this and Sections 6.6 and 6.7 that this condition is fulfilled, that is, $\tilde{\varepsilon}'_m < 0$ and $\kappa \ll 1$.

It is convenient to represent the Hamiltonian $\mathcal{H}$ as a sum of two Hermitian Hamiltonians $\mathcal{H} = \mathcal{H}' + i\kappa\mathcal{H}''$, where the term $i\kappa\mathcal{H}''$ ($\kappa \ll 1$) represents losses in the system. The Hamiltonian $\mathcal{H}'$ formally coincides with the Hamiltonian of the problem of metal–insulator transition (Anderson transition) in quantum systems [65–68]. More specifically, the Hamiltonian $\mathcal{H}'$ maps the quantum mechanical Hamiltonian for the Anderson transition problem with both on- and off-diagonal correlated disorder. Since the off-diagonal matrix elements in $\mathcal{H}'$ have different signs, the Hamiltonian is similar to the so-called gauge-invariant model. This model in turn, is a simple version of the random flux model, which represents a quantum system with random magnetic field [65] (see also recent numerical studies [69–71]). Hereafter, we refer to operator $\mathcal{H}'$ as to Kirchhoff's Hamiltonian (KH).

Thus, the problem of the field distribution in the system, that is, the problem of finding a solution to Kirchhoff's Eq. (6.61), becomes an eigenfunction problem for the KH, $\mathcal{H}'\Psi_n = \Lambda_n\Psi_n$, whereas the losses can be treated as perturbations. Since the real part ε'_m of the metal dielectric function $\tilde{\varepsilon}_m$ is negative ($\tilde{\varepsilon}'_m < 0$) and the permittivity of the dielectric host is positive ($\tilde{\varepsilon}_d > 0$), the manifold of the KH eigenvalues Λ_n contains eigenvalues that have the real parts equal (or close) to zero. Then, eigenstates Ψ_n that correspond to eigenvalues $|\Lambda_n/\tilde{\varepsilon}_m| \ll 1$ are strongly excited by the external field and seen as giant field fluctuations representing the resonant surface plasmon modes. If we assume that the eigenstates excited by the external field are localized, they should look like local-field peaks. The average